ACS APPLIED MATERIALS & INTERFACES

Research Article

www.acsami.org

Reduction-Cleavable Polymeric Vesicles with Efficient Glutathione-Mediated Drug Release Behavior for Reversing Drug Resistance

Tianbin Ren,[†] Wei Wu,[†] Menghong Jia,[†] Haiqing Dong,[†] Yongyong Li,*[,†] and Zhouluo Ou[‡]

[†]The Institute for Biomedical Engineering and Nano Science, School of Materials and Engineering, Tongji University, Shanghai 200092, P. R. China

[‡]Breast Cancer Institute, Cancer Hospital, Department of Oncology, Shanghai Medical College, Fudan University, Shanghai 200032, P. R. China

Supporting Information

ABSTRACT: In the treatment of cancer, multidrug resistance (MDR) has been the major obstacle to the success of chemotherapy. The underlying mechanism relies on the overexpression of drug-efflux transporters that prevent the intracellular transport of the drug. In this study, reduction-cleavable vesicles were designed and developed with efficient glutathione-mediated drug-release behavior for reversing drug resistance. Polymeric vesicles were self-assembled from triblock copolymers with disulfide-bond-linked poly(ethylene glycol) (PEG) and poly(ε-benzyloxycarbonyl-L-lysine) (PzLL). Observations from transmission electron microscopy (TEM) and confocal laser scanning microscopy (CLSM) outline an obvious hollow structure surrounded by a thin outer layer, indicating the successful formation of the vesicles. Using fluorescently detectable doxorubicin hydrochloride (DOX·HCl) as the model drug, a significant acceleration of drug release regulated by glutathione (GSH) was found (>3-fold difference). Upon incubation of the DOX·HCl-loaded polymeric vesicles with the HeLa cervical cancer cell line exposed to glutathione, an enhanced nuclear accumulation of DOX·HCl was observed, elicited by the preferred disassembly of the vesicle structure under reducing conditions. Importantly, by using the gemcitabine hydrochloride (GC·HCl)-resistant breast cancer cell line MDA-MB-231, it was found that cell viability was significantly reduced after treatment with GC·HCl-loaded polymeric vesicles, indicating that these vesicles can help to reverse the drug resistance.

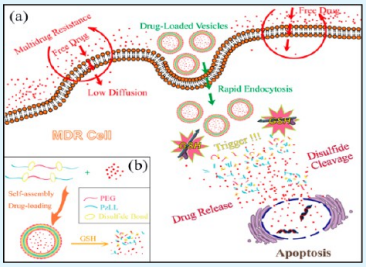

KEYWORDS: *reduction cleavable, polymeric vesicles, multidrug resistance, anticancer drug*

1. INTRODUCTION

Chemotherapy is currently a predominant but far from satisfying method to treat cancer. The efficacy of a chemotherapeutic drug is often compromised by the occurrence of multidrug resistance (MDR) in the cancer. Statistical data indicated that quite a large proportion of patients eventually die as a result of MDR, making it one of the leading causes of cancer-mediated mortality.[1,2] Research into MDR revealed that the underlying mechanism is generally associated with the upregulation of drug efflux transporters (e.g., P-glycoprotein (ABCB1), ABCC1, ABCG2, etc.), which have been the major obstacle to the success of chemotherapy. A variety of strategies have been proposed so far to deal with MDR, including direct inhibition of the overexpression of drug transporters, gene silencing, transcriptional regulation, and drug encapsulation.[1−5] Among the reported strategies, drug encapsulation using polymeric nanoparticles has been developed as an efficient strategy to address the critical issue of MDR.[6−8] The shield effect for the recognition of MDR transporters by cancer cells is the key route to overcome MDR, which eventually results in an effective intracellular drug concentration inside the cells.

Toward this end, nanoparticles have shown great advantages, including prolonged circulation time, reduced nonspecific uptake, passive/active accumulation at the sites of tumors, controlled drug-release behavior, active targeting potential, and so forth.[9,10] Polymeric micelles and vesicles (also referred to polymersomes) represent two types of widely studied drug-delivery systems (DDS).[11−13] Polymeric micelles are generally defined as polymeric nanoparticles with a core−shell structure self-assembled from amphiphilic polymers, whereas polymeric vesicles usually denote nanoparticles with a hollow structure surrounded by a bilayered membrane.[14] Currently, most of the reported polymeric nanoparticle to address the issue of MDR focus on polymeric micelles. For example, Lai et. al observed a significant inhibition of P-gp activity of MCF-7/ADR cells by using doxorubicin-loaded poly(L-lactide)-vitamin E TPGS (PLA-TPGS) micelles as hydrophobic drug-delivery vehicles.[8] Wang and co-workers engineered redox-responsive micelles based on a disulfide-bond-linked block polymer of poly(ε-caprolactone) and poly(ethyl ethylene) phosphate (PCL-SS-PEEP). It was found that these micelles helped to enhance drug accumulation in drug-resistant cells, resulting in an obviously higher growth inhibition of MDR cancer cells.[15] In contrast to micelles, the typical hollow structure of vesicles makes them a versatile platform to carry not only hydrophobic drugs within the aqueous interior cavities but also hydrophilic drugs within

Received: July 17, 2013
Accepted: October 2, 2013
Published: October 2, 2013

the bilayered membrane. However, there are relatively few reports concentrating on the development of polymeric vesicles to overcome MDR.

To optimize the therapeutic effects, it is favorable to selectively and rapidly release the carried drugs at the target sites. The utilization of drug-delivery system (DDS) with triggering mechanisms for drug release is an effective strategy.[16] Those stimuli designed for triggering release include temperature, pH, redox potential, light, ultrasound, and magnetic field.[11] Redox potential, as an appealing stimulus, holds the advantage of the concentration gradient between the intracellular and extracellular redox potentials that is regulated by glutathione (GSH). Intracellular GSH maintains a millimolar concentration in the cytosol and subcellular compartments, whereas in plasma GSH concentrations are found at lower levels (micromolar) because of rapid enzymatic degradation.[17−19] Furthermore, the concentration of GSH in many tumors has been reported to be 4-fold higher than that of normal tissue because of the reducing and hypoxic nature of the tumor.[20] Many reports revealed that disulfide bonds tend to undergo rapid cleavage into free thiols when exposed to a reductive environment. For example, Hubbell and co-workers reported a highly sensitive and very rapid-reacting drug-delivery system based on disulfide-bond-linked poly(ethylene glycol) (PEG) and poly(propylene sulfide) (PPS) (PEG-SS-PPS).[21] In the past few years, our group has also harnessed the property of the cleavable disulfide bond to engineer polymeric micelles, polyplexes, for drug and gene delivery.[17,22,23] These nanoparticles have a common feature that includes a PEG-sheddable shell with a redox-sensitive disulfide linkage that disassemble rapidly to accelerate drug release or improve transfection efficiency under intracellular tumor-relevant glutathione (GSH) levels.

In our previous work, polypeptide was a major polymer that constituted the nanoparticles in addition to PEG. Polypeptides are desired building blocks for polymeric nanoparticles because of their stimuli-responsiveness, functionalities, hierarchy assembly, and biocompatibility. In a recent review on stimuli-responsive polymeric vesicles, Li and Keller foresaw that a PEG-polypeptide would be a good candidate to engineer polymeric vesicles.[24] Herein, we designed and developed a disulfide-bridged amphiphilic triblock copolymer of poly(ethylene glycol) (PEG) and poly(ε-benzyloxycarbonyl-L-lysine) (PzLL) (PzLL-SS-PEG-SS-PzLL) that can self-assemble into vesicles (Figure 1). These vesicles were engineered with a redox-responsive property that allows for the regulation of drug release via glutathione. This glutathione-mediated drug-release behavior was then harnessed to overcome the drug resistance of cancer cells by using gemcitabine hydrochloride (GC·HCl)-resistant MDA-MB-231 cells as the model.

2. EXPERIMENTAL SECTION

Materials. α,ω-Dipropionic acid poly(ethylene glycol) (HOOC-PEG-COOH, M_n = 2000, Shanghai Yare Biotech, Inc.), ε-benzyloxycarbonyl-L-lysine (zLL, GL Biochem, Ltd), triphosgene (99%, Sigma-Aldrich), cystamine dihydrochloride (Sigma-Aldrich), *N*-(3-dimethylaminopropyl)-*N*′-ethylcarbodiimide hydrochloride (EDC·HCl, Aladdin), *N*-hydroxysuccinimide (NHS, Aladdin), fluorescein isothiocyanate (FITC, Aladdin), doxorubicin hydrochloride (DOX·HCl, Zhejiang Hisun Pharmaceutical Co., Ltd), gemcitabine hydrochloride (GC·HCl, Gemzar, lot no. A875303A, Lilly), Dulbecco's modified Eagle's medium (DMEM, Gibco Invitrogen Corp.), fetal bovine serum (FBS, Gibco Invitrogen Corp.), penicillin/streptomycin (Gibco Invitrogen Corp.), trypsin (Gibco Invitrogen Corp.), Dubelcco's phosphate-buffered saline (DPBS, Gibco Invitrogen Corp.), 3-(4,5-dimethylthiazol-2-yl)-2,5-diphenyltetrazolium bromide (MTT, Gibco Invitrogen Corp.), paraformaldehyde (4%, DingGuo Chang Sheng Biotech. Co., Ltd.), Leibovitz's L-15 (Shanghai Usen Biological Technology Co., Ltd.), Cell Cycle and Apoptosis Analysis Kit (Beyotime Institute of Biotechnology) were purchased and used as received. Tetrahydrofuran (THF, SCRC), dichloromethane (DCM, SCRC), and *N*,*N*-dimethyl formamide (DMF, SCRC) were used after a drying process. The HeLa human cervical cancer cell line was supplied by the Cell Center of the Cancer Hospital at Fudan University and was cultured with DMEM containing 10% FBS and 0.1% (v/v) penicillin/streptomycin in a humidified atmosphere with 5% (v/v) CO_2 at 37 °C. Human breast cancer cell line MDA-MB-231 (HTB-26) was from the Breast Cancer Institute of the Cancer Hospital at Fudan University and was cultured under the same conditions as HeLa cells except for the use of L15 culture media.

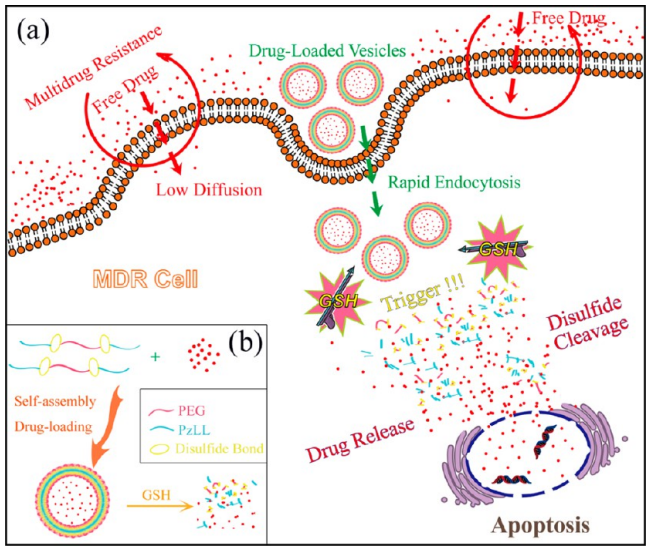

Figure 1. (a) Schematic illustration of redox-responsive polymeric vesicles for overcoming the multidrug resistance of cancer cells and (b) schematic outline of the predicted self-assembly behavior of PzLL-SS-PEG-SS-PzLL triblock copolymers and their drug-release behavior.

Synthesis of Amino-Terminated Poly(ethylene glycol) (NH_2-SS-PEG-SS-NH_2). Cystamine dihydrochloride (8.88 mmol) in 30 mL of deionized water was desalinated by NaOH under continuous stirring at rt for 3 h. Cystamine was then collected by rotary evaporation. The residue was then dissolved in CH_2Cl_2 and subjected to a filtration process to exclude the insoluble matter. Cystamine was obtained after CH_2Cl_2 removal by rotary evaporation followed by an overnight vacuum-drying process. HOOC-PEG-COOH (0.4 mmol) was dissolved in 15 mL of dry CH_2Cl_2, and the mixture of 0.47 mmol of EDC·HCl and 0.47 mmol of NHS dissolved by 5 mL dry CH_2Cl_2 was added gradually. After stirring under a N_2 atmosphere for about 12 h at rt, the mixture was dropped into a solution of cystamine in 10 mL of CH_2Cl_2. The reaction proceeded under N_2 at rt for 24 h. The product was then collected by vacuum rotary evaporation and subjected to a dialysis procedure (MWCO = 1.0 kDa) after being dissolved in 5 mL of THF. Finally, the desired NH_2-SS-PEG-SS-NH_2 was obtained by freeze-drying the solution for further use.

Synthesis of ε-Benzyloxycarbonyl-L-lysine *N*-Carboxyanhydride (Z-Lys NCA). A solution of 9 mmol triphosgene in 30 mL of THF was added dropwise to 60 mL of THF suspended with ε-benzyloxycarbonyl-L-lysine (10 mmol). The resultant solution was heated at 50 °C under a N_2 atmosphere with continuous stirring. After about 3 h, when the solution gradually became clear, the solvent THF was reduced to about 10 mL by vacuum rotary evaporation treatment. The mixture was carefully dropped into 150 mL of cold *n*-hexane for crystallization. The procedure was performed twice before the product was vacuum-dried at rt overnight.

Synthesis of PzLL-SS-PEG-SS-PzLL. Triblock copolymer PzLL-SS-PEG-SS-PzLL was synthesized by ring-opening polymerization (ROP) of Z-Lys NCA in dry *N*,*N*-dimethylformamide (DMF) with NH_2-SS-PEG-SS-NH_2 as the initiator. Two different block polymers were synthesized by varying the feed ratio of NH_2-SS-PEG-SS-NH_2 and Z-Lys NCA from 2:1 to 1:2. The reaction was performed under a N_2 atmosphere at rt for 72 h, and the desired product was obtained by freeze-drying after purification by dialysis against distilled water.

Synthesis of FITC-Labeled PzLL-SS-PEG-SS-PzLL. Fluorescein isothiocyanate (FITC) was conjugated to PzLL-SS-PEG-SS-PzLL for fluorescent microscopy evaluation. A mixture of 30 mg of PzLL-SS-PEG-SS-PzLL and 30 mg of FITC in 5 mL of anhydrous DMF with a small amount of triethylamine (Et_3N) was placed under continuous stirring at rt for 48 h, and then the desired FITC-PzLL-SS-PEG-SS-PzLL conjugate was obtained by freeze-drying after dialysis for further use.

Self-Assembly of the Copolymer into Polymeric Vesicles. To prepare the polymeric vesicles, 3.0 mg of PzLL-SS-PEG-SS-PzLL was dissolved in 3.0 mL of THF, and 6.0 mL of deionized water was dropped into the copolymer solution for 2 h by a peristaltic pump (BQ50S) with continuous stirring. The mixture was then dialyzed against deionized water to remove the solvent THF for 2 days by changing the water three times each day.[25]

Characterization. FTIR spectra of the samples were obtained on a Bruker Tensor 27 spectrometer. ^{1}H NMR spectra were obtained by a Bruker DMX-500 NMR spectrometer using DMSO-d_6 as the solvent.

The molecular weight was analyzed using an Applied Biosystems 4700 Proteomics (TOF/TOF) Analyzer following the protocol described in an earlier work.[26]

The size and distribution of polymeric vesicles were measured with dynamic light scattering (DLS) at 25 °C using Nano-ZS 90 Nanosizer (Malvern Instruments). The vesicles morphology was determined with a transmission electron microscope (TEM) using a Hitachi H7100 (Hitachi, Ltd.). The samples were stained with phosphotungstic acid (1 wt %) before observation.

The critical aggregation concentration (CAC) of the copolymer was measured using pyrene, which is a hydrophobic florescence probe and so preferably locates in the membrane. In detail, 25 μL of pyrene solution in acetone ($\approx$6 μM) was added into 4 mL centrifuge tubes, and acetone was removed by evaporation under an ambient atmosphere. Subsequently, the polymeric vesicles (2 mL in distilled water) with concentration ranging from 0.05×10^{-3} to 0.5 mg/mL were added to the pyrene-containing centrifuge tube with the concentration of pyrene kept the same. After sonication for 10 min, the solution was placed in a dark shaker at rt for 1 day to make the pyrene reach an equilibration before measurements were taken. The fluorescence spectra were recorded with the emission (EM) wavelength set at 393 nm (Hitachi F-2500 luminescence spectrometer). The excitation fluorescence (EX) was monitored at 338 and 333 nm, respectively. The CAC was correlated to the concentration of the cross-point by extrapolating the intensities of I_{338}/I_{333} at ranges of low and high concentration.

Three milligrams of PzLL-SS-PEG-SS-PzLL was dissolved in 3.0 mL of nile red/THF (0.3 mg/L), and 6.0 mL of deionized water was dropped into the copolymer solution followed by the addition of 100 μL of 5(6)-carboxyfluorescein/deionized water (0.05 mg/mL) with continuous stirring for 2 h. Free dye and THF were then removed by dialysis (MWCO 1.0 kDa). Fluorescence images were acquired on a confocal microscope (Leica TCS SP5 II).

Encapsulation and in Vitro Release of DOX·HCl. Six milligrams of PzLL-SS-PEG-SS-PzLL was dissolved in 10 mL of THF by a method described above, resulting in the polymeric vesicles. Afterwards, the aqueous solution of DOX·HCl/PBS buffer (pH 7.4, 10 mM) (6 mg/3 mL) was added while stirring was maintained in the following 12 h under dark conditions. The DOX·HCl-loaded polymeric vesicles were formed after a dialysis process to remove free DOX·HCl (MWCO = 3.5 kDa). The amount of unloaded drugs in the dialysate was quantitatively measured by a UV−vis spectrophotometer (Varian). The entrapment efficiency (EE) and drug-loading efficiency (DL) were estimated according to the following equations[27]

$$\mathrm{EE}\ (\%) = \left(\frac{\text{mass of DOX·HCl in vesicles}}{\text{mass of DOX·HCl fed initially}}\right)\times 100$$

$$\mathrm{DL}\ (\%) = \left(\frac{\text{mass of DOX·HCl in vesicles}}{\text{mass of DOX·HCl loaded vesicles}}\right)\times 100$$

The release of DOX·HCl from polymeric vesicles was evaluated using a dialysis method (MWCO = 8−14 kDa). Briefly, 2 mL of DOX·HCl-loaded polymeric vesicle suspensions (0.25 mg/mL) was dialyzed against 30 mL of PBS (pH 7.4, 10 mM) containing 10 mM GSH and 30 mL of PBS (pH 7.4, 10 mM) without GSH at 37 °C, respectively. At specific time points, samples were collected and measured immediately on a UV−vis spectrophotometer and then immediately poured back and kept at 37°C. The release experiments were done in triplicate.

Cytotoxicity Test in HeLa Cells. Cell viability in the absence and presence of both PzLL-SS-PEG-SS-PzLL vesicles and DOX·HCl-loaded PzLL-SS-PEG-SS-PzLL vesicles was evaluated using the MTT (3-(4, 5-dimethylth iazol-2-yl)-2,5-diphenyl tetrazolium bromide) assay. For the experiments, HeLa cells were seeded at a density of 5000 cells/well in 200 μL of DMEM in a 96-well plate. After the attachment period, polymeric vesicles 2 was added to yield the gradient concentrations ranging from 15.6 to 250 mg/L and was incubated for 24 h with the cells. At the end of the incubation, 20 μL of a 5 mg/mL sterile filtered MTT solution in DPBS was added in each well. Afterwards, the plate was incubated for 4 h in the incubator. After the addition of 150 μL of DMSO into each well, the plate was placed on a dark shaking platform at rt for 5 min before measuring the optical density (OD) at λ = 492 nm using a Multiscan MK3 plate reader (Thermo Fisher Scientific). Relative cell viability (%) was obtained based on the equation below

$$\text{cell viability}\ (\%) = \left(\frac{\mathrm{OD_{treated}}}{\mathrm{OD_{control}}}\right)\times 100$$

where $OD_{treated}$ was obtained with treated wells containing DOX·HCl-loaded polymeric vesicles, and the $OD_{control}$ was obtained with control wells containing only DMEM.[28]

GSH Sensitivity Test. To validate the influence of GSH on DOX·HCl release, HeLa cells were seeded at a density of 5000 cells/well in 200 μL of DMEM in a 96-well plate. After a 24 h attachment period, the cells were cultured for another 7 h with various concentrations of DOX·HCl-loaded polymeric vesicles 2 ranging from 15.6 to 250 mg/L in DMEM. The cells were then rinsed with DPBS, and some specific wells of the fresh cell culture media were treated with 10 mM GSH for an additional 3 h. Cells in the absence of GSH used as the control were also treated with MTT.

The intracellular DOX·HCl release behavior and internalization were characterized by LSCM. Specifically, HeLa cells were seeded at a density of 2×10^5 cells/well in 1 mL of DMEM in a 6-well plate. After 24 h of attachment culture, the cells were treated with DOX·HCl-loaded polymeric vesicles at concentrations ranging from 15.6 to 62.5 mg/L for 5 h and then rinsed with DPBS three times. Of the six wells of cells, the three wells incubated with different concentrations were treated with 10 mM GSH for an additional 2 h and the others were untreated. After the cells were rinsed three times with DPBS, 4% paraformaldehyde was added, and the cells were kept at rt for 15 min. 40-6-Diamidino-2-phenylindole (DAPI, blue) (200 μL, 5 mg/L) was then added to stain the nuclei for an additional 15 min. The cells were washed three times again with DPBS, and then observed using CLSM.[29]

Qualitative and Quantitative Endocytosis Analysis of Polymeric Vesicles. Qualitatively, the cellular uptake of FITC-labeled PzLL-SS-PEG-SS-PzLL vesicles 2 was monitored on a fluorescence microscope (Nikon ECLIPSE 80i) at different times. More specifically, HeLa cells were seeded at a density of 2×10^5 cells/well in 1 mL of DMEM in a 6-well plate followed by 24 h of adherent

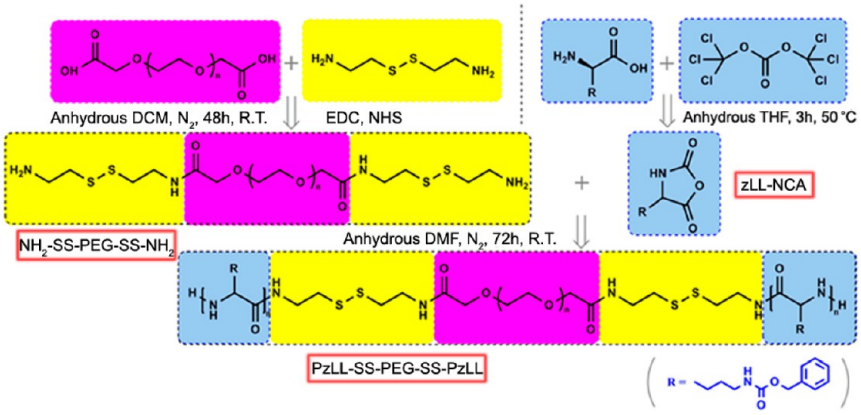

Figure 2. Illustration of the synthetic route of PzLL-SS-PEG-SS-PzLL triblock copolymers.

culture. After renewing the culture medium, the cells were coincubated with FITC-labeled PzLL-SS-PEG-SS-PzLL polymeric vesicles 2 suspensions (250 mg/L). The fluorescence intensity was imaged at 30 min, 1 h, 2 h, and 5 h.

Quantitatively, the endocytosis rate of FITC-labeled PzLL-SS-PEG-SS-PzLL polymeric vesicles 2 was evaluated by flow cytometry analysis (FACS). Briefly, HeLa cells were seeded at a density of 2×10^5 cells/well in 1 mL of DMEM in a 6-well plate. After a 24 h attachment period, the cells were cultured with FITC-labeled PzLL-SS-PEG-SS-PzLL polymeric vesicles (250 mg/L) in fresh DMEM for different periods ranging from 30 min to 5 h. Then the cells were rinsed with DPBS twice and suspended in 500 μL of 2% paraformaldehyde for analyses with a flow cytometer (FACScan).

Endocytic Pathway of Polymeric Vesicles 2 in Drug-Resistant MDA-MB-231 Cells. Drug-resistant MDA-MB-231 cells were seeded at a density of 5000 cells/well in 96-well plates and cultured at 37 °C in 5% CO_2 for 24 h. To evaluate the mechanisms of vesicles uptake, MDA-MB-231 cells were preincubated with different inhibitors, such as the metabolic inhibitor sodium azide (10 mM), endocytosis inhibitor chlorpromazine (10 mg/L), genistein (200 mg/L), and colchicine (5 mg/L), for 30 min prior to FITC-labeled PzLL-SS-PEG-SS-PzLL polymeric vesicles (250 mg/L) application and the cells were incubated for 2 h for the uptake experiment under the same culture conditions. The cells without preincubation with an inhibitor were set as the control. The results are presented as the relative uptake percentage.[30]

Cytotoxicity Studies in Gemcitabine Hydrochloride (GC·HCl)-Resistant MDA-MB-231 Cells. To investigate the cytotoxicity of GC·HCl with or without encapsulation into PzLL-SS-PEG-SS-PzLL polymeric vesicles, drug-resistant MDA-MB-231 cells were seeded at a density of 5000 cells per well into 96-well plates and cultured for 24 h. The free GC·HCl or PzLL-SS-PEG-SS-PzLL polymeric vesicles or GC·HCl-loaded PzLL-SS-PEG-SS-PzLL polymeric vesicles were added to reach final concentrations of 15.6−500 mg/L in 100 μL at 37°C. Cytotoxicity was determined after a 20 h incubation. MTT assay was performed by following the same procedure described above for characterizing the viability of the Hela cells.

To evaluate this effect visually, drug-resistant MDA-MB-231 cells were seeded at a density of 80 000 cells/well in a 6-well plates and cultured for 24 h. Free GC·HCl or GC·HCl-loaded PzLL-SS-PEG-SS-PzLL polymeric vesicles were added to reach final concentrations of 15.6−125 mg/L in a volume of 1.5 mL at 37°C for 12 h. The cells growth status was then observed by microscope (Motic AE2000), and the cells were rinsed with DPBS twice and suspended in 500 μL of 2% paraformaldehyde for analyses.

3. RESULTS AND DISCUSSION

Synthesis and Characterization of Triblock Copolymer PzLL-SS-PEG-SS-PzLL. The triblock copolymer PzLL-SS-PEG-SS-PzLL is structured with PEG and PzLL blocks bridged by a disulfide bond. The selective cleavable property of disulfide bond upon redox environment allows the structural control of the triblock copolymer. The link from the disulfide bond enables the disassembly of the hollow structure under the intracellular tumor-relevant GSH concentration, thus facilitating the drug release inside the cells. This structural disassembly could be harnessed for the selective release of the drug to overcome MDR and thus augment the intracellular accumu-

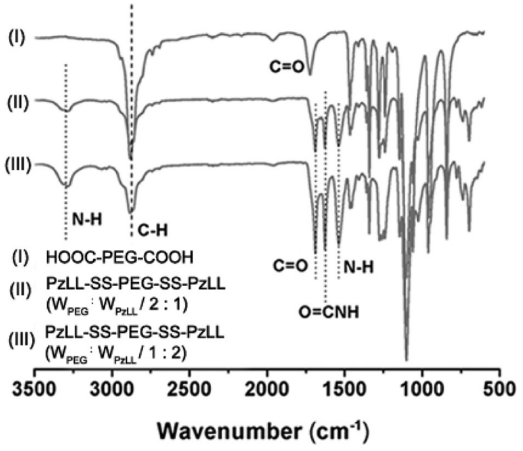

Figure 3. FTIR spectra of intermediates and products: (I) HOOC-PEG-COOH, (II) PzLL-SS-PEG-SS-PzLL (W_{PEG}/W_{PzLL} 2:1), and (III) PzLL-SS-PEG-SS-PzLL (W_{PEG}/W_{PzLL} 1:2).

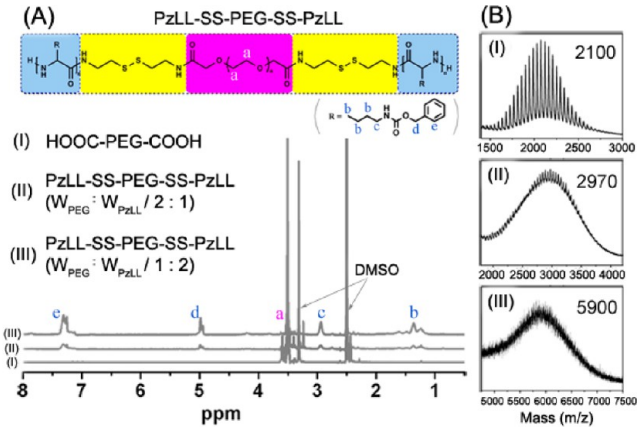

Figure 4. Spectroscopic analysis of triblock copolymers. Representative ^{1}H NMR spectra are summarized in panel A. The mass spectra are shown in panel B.

Table 1. Composition and Physicochemical Characteristics of PzLL-SS-PEG-SS-PzLL Copolymers

copolymer	$M_{n\ design}$	M_n[a]	M_n[b]	size (PDI)[c]	CAC (mg/L)[d]
PzLL-SS-PEG-SS-PzLL 1	3000	2950	2970		
PzLL-SS-PEG-SS-PzLL 2	6000	5300	5900	380 (0.25)	14

[a]Determined by ^{1}H NMR. [b]Determined by MS. [c]Determined by DLS. [d]CAC denotes the critical aggregation concentration

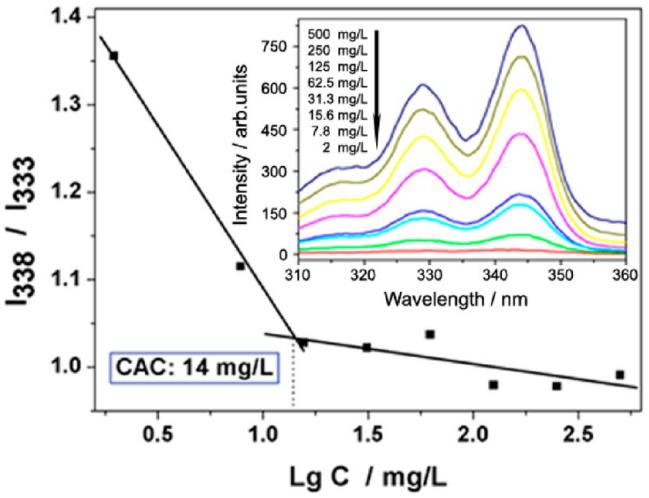

Figure 5. CAC fluorescence excitation spectra of pyrene with polymeric vesicles 2.

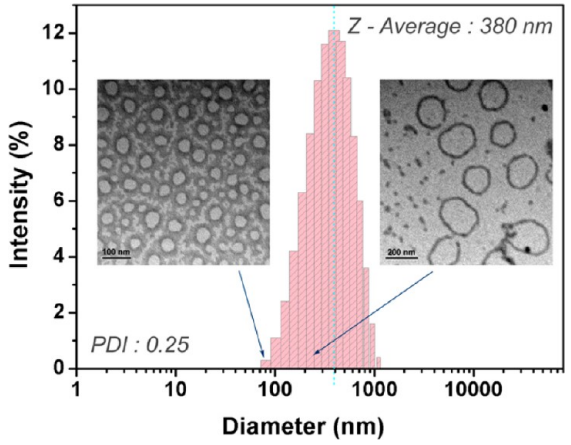

Figure 6. Size distribution and morphology of PzLL-SS-PEG-SS-PzLL (W_{PEG}/W_{PzLL} 1:2) vesicles determined by DLS and TEM (inset).

lation of the drugs. PzLL-SS-PEG-SS-PzLL is afforded by ROP of Z-Lys NCA with NH_2-SS-PEG-SS-NH_2 as the initiator, as shown in Figure 2. The ROP of amino acid-*N*-carboxyanhydrides (NCA) represents the most commonly applied technique to produce polypeptides and hybrid polypeptides on a several gram scale.[31−33] In this study, two different block polymers were obtained by varying the feed ratio of NH_2-SS-PEG-SS-NH_2 and Z-Lys NCA from 2:1 to 1:2.

The desired structures of PzLL$_n$-SS-PEG-SS-PzLL$_n$ products were confirmed by spectroscopic analysis. FTIR spectra show the stretching vibration of N−H at 3287 cm^{-1} and a strong absorbance band at 1731 cm^{-1} associated with C═O stretching vibration (Figure 3). The ^{1}H NMR spectra in DMSO-d_6 are

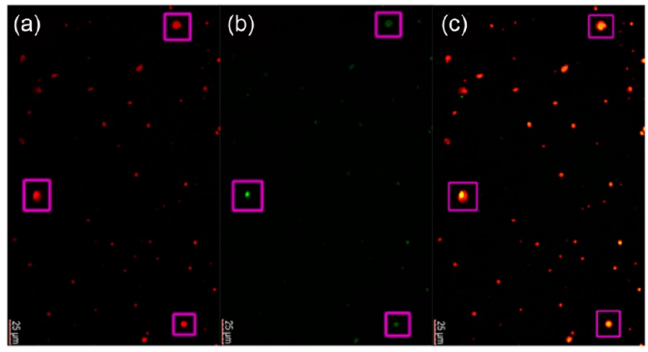

Figure 7. CLSM micrographs of polymeric vesicles 2 loaded with nile red (hydrophobic) and 5(6)-carboxyfluorescein (hydrophilic). (a) Nile red, (b) 5(6)-carboxyfluorescein, and (c) overlay panels A and B.

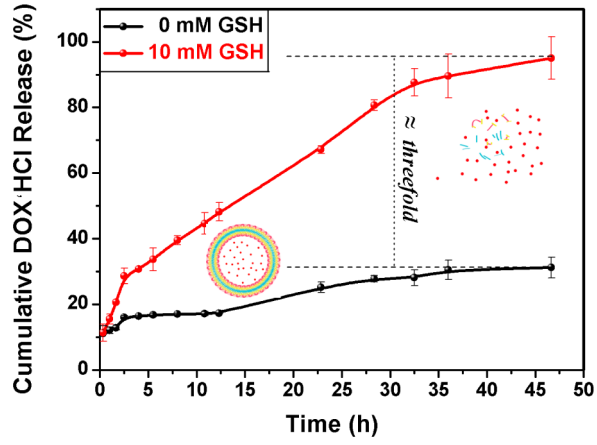

Figure 8. In vitro DOX·HCl release from polymeric vesicles in the presence and absence of GSH in PBS (pH 7.4). Data are presented as the mean ± SD (n = 3).

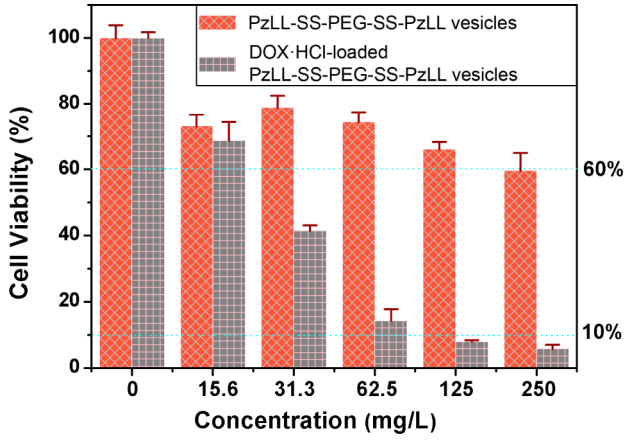

Figure 9. Dose-dependent cytotoxicity of PzLL-SS-PEG-SS-PzLL polymeric vesicles 2 alone and DOX·HCl-loaded PzLL-SS-PEG-SS-PzLL polymeric vesicles 2 after a 24 h coincubation. Data are presented as the mean ± SD (n = 5).

shown in Figure 4A in which the resonance peak from the PEG moiety (δ = 3.52 ppm) and the PzLL fragment (δ = 1.32−1.77, 2.96, 4.99, and 7.34 ppm) are observed.[17] The relative molecular mass is estimated by integrating signals form all methylene (δ = 3.52 ppm) and phenyl protons (δ = 7.34 ppm). The mass spectrometry data reveals two triblock copolymers with M_n = 2970 or 5900 (Figure 4B), which are close to the

dx.doi.org/10.1021/am402860v | ACS Appl. Mater. Interfaces 2013, 5, 10721−10730

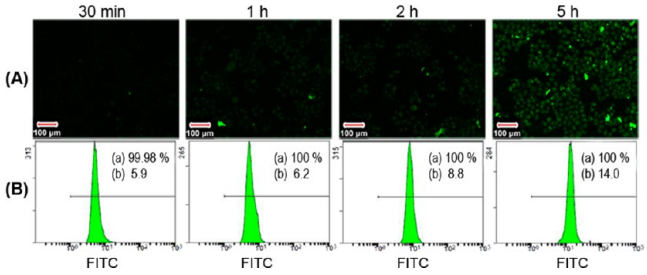

Figure 10. Cellular uptake of FITC-labeled PzLL-SS-PEG-SS-PzLL polymeric vesicles 2 in 5 h by (A) fluorescence microscopy and (B) flow cytometry. (a) Cell uptake rate (%) and (b) mean fluorescence intensity.

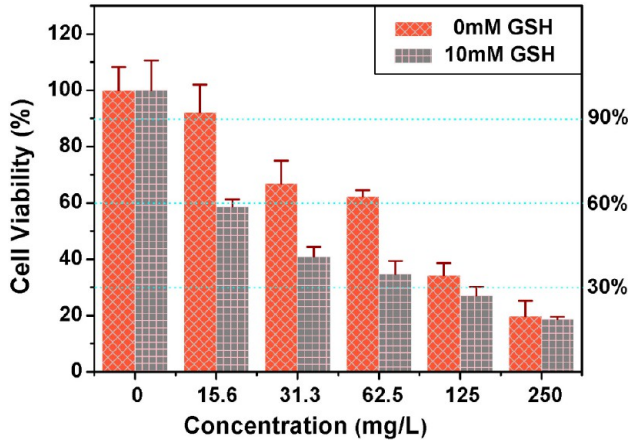

Figure 11. Cytotoxicity of DOX·HCl-loaded PzLL-SS-PEG-SS-PzLL polymeric vesicles 2 in the presence and absence of GSH at different concentrations of vesicles. Data are presented as the mean ± SD (n = 5).

calculated M_n by ^{1}H NMR (Table 1). The two triblock copolymers synthesized under different conditions are PzLL-SS-PEG-SS-PzLL 1 for M_n 2970 and PzLL-SS-PEG-SS-PzLL 2 for M_n 5900, corresponding to the weight ratio of PEG and PzLL of 2:1 and 1:2, respectively.

Preparation and Physical Chemical Properties of PzLL-SS-PEG-SS-PzLL Polymeric Vesicles. The "solvent-switch" method was applied to engineer polymeric vesicles from the above two synthesized triblock copolymers. The critical aggregation concentration (CAC) is measured as 14 mg/L for PzLL-SS-PEG-SS-PzLL 2 (W_{PEG}/W_{PzLL} 1:2) using pyrene as a fluorescence probe (Figure 5), although it can not yield a CAC value for PzLL-SS-PEG-SS-PzLL 1 (W_{PEG}/W_{PzLL} 2:1) because of its improper amphiphilic nature. Therefore, the following study focuses on PzLL-SS-PEG-SS-PzLL 2, and the term polymeric vesicles 2 denotes vesicles prepared from the PzLL-SS-PEG-SS-PzLL 2.

The dynamic light scattering (DLS) measurement of polymeric vesicles 2 shows an average diameter of 380 nm and a relatively wide size distribution (PDI 0.25). TEM analysis further confirms the formation of vesicles, as indicated by the hollow structure during observation. In line with the DLS detection, TEM images show that vesicles with a relatively small size are concomitant with those vesicles with a large size (> 200 nm), leading to a somewhat wide distribution of the vesicles (Figure 6). Vesicles with different sizes are also captured in one TEM image under the same condition, as shown in Figure S1.

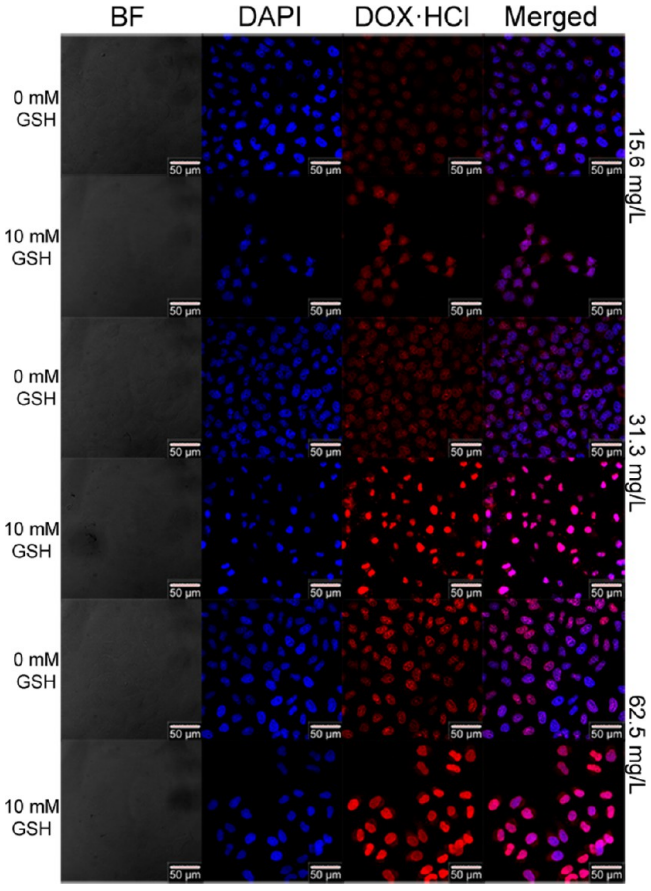

Figure 12. GSH-induced intracellular drug delivery. Fluorescent images of intracellular delivery of DOX·HCl (red) from PzLL-SS-PEG-SS-PzLL polymeric vesicles 2 to HeLa cells in the absence and presence of GSH, respectively. The concentrations of polymeric vesicles 2 ranged from 15.6 to 62.5 mg/L.

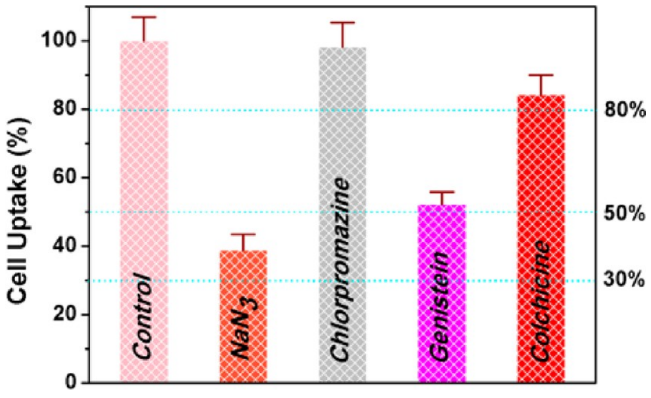

Figure 13. Cellular uptake percentage of FITC-labelled PzLL-SS-PEG-SS-PzLL polymeric vesicles 2 in drug-resistant MDA-MB-231 cells following preincubation with various endocytic inhibitors. Data are presented as the mean ± SD (n = 3).

To confirm the structure of the polymeric vesicles further, CLSM of the prepared giant polymeric vesicles specially loaded with nile red (red, hydrophobic) and 5(6)-carboxyfluorescein (green, hydrophilic) clearly shows the hollow structure. A faster mixing process was conducted in an attempt to yield vesicles with a larger size on the microscale level because nanoscaled vesicles could not be observed by optical microscopy. In the overlay of the red and green images, the three selected vesicles

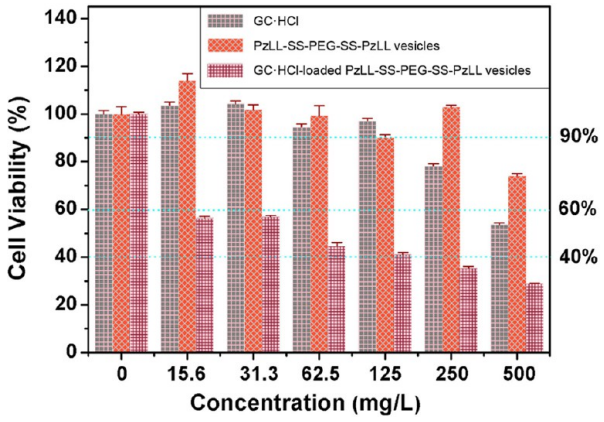

Figure 14. Dose-dependent cytotoxicity of GC·HCl alone, PzLL-SS-PEG-SS-PzLL polymeric vesicles 2 alone, and GC·HCl-loaded PzLL-SS-PEG-SS-PzLL polymeric vesicles 2 after 24 h coincubation with drug-resistant MDA-MB-231 cells. Data are presented as the mean ± SD (n = 3).

with a larger size obviously demonstrate a different spatial distribution of the fluorescence, where red locates outward in comparison with yellow. Yellow fluorescence is arising from the overlap of nile red and 5(6)-carboxyfluorescein because some nile red exists in the inner cavity. This observation indicates the existence of a hydrophilic hollow inner cavity stained by the hydrophilic 5(6)-carboxyfluorescein and a hydrophobic bilayer membrane stained by the hydrophobic nile red (Figure 7).

Drug Loading and Release Behavior Triggered by GSH. The hydrophilic anticancer drug DOX·HCl can be loaded into polymeric vesicles 2 within the aqueous interior cavities. In our experiments, the feed ratio of polymeric vesicles 2 and DOX·HCl is 1:1. Polymeric vesicles 2 yield a 21% drug-loading efficiency and 21% entrapment efficiency. The kinetics of the release of DOX·HCl from polymeric vesicles 2 with or without exposure to GSH in PBS (pH 7.4) are shown in Figure 8. In the first 3 h, a fast release rate is observed followed by a near linear slow release for both release curves. Specifically, in the absence of GSH, only 30% of DOX·HCl is released in 48 h; however, over 90% of DOX·HCl is released in the same period in the presence of 10 mM GSH, which is 3-fold of that without GSH owing to the disassembly of PzLL-SS-PEG-SS-PzLL polymeric vesicles with disulfide bond cleavage. The disruption of the vesicles triggered by GSH can be clearly supported by the fact of that precipitates occur gradually after GSH exposure of the sample, as seen by the naked eye (inset in Figure S2). Meanwhile, the group without GSH exposure remains stable. Moreover, the TEM image clearly shows aggregated assemblies formed by hydrophobic PzLL segments detached from vesicles after triggering by GSH (Figure S2), which is in line with the phenomenon observed above.

In Vitro Cytotoxicity of Blank and DOX·HCl-Encapsulated Vesicles. An acceptable safety margin and therapeutic efficacy are two of the critical factors to attain clinical success with synthetic drug-delivery carriers. In our study, the cytotoxicity of the PzLL-SS-PEG-SS-PzLL polymeric vesicles 2 and DOX·HCl loaded vesicles 2 against HeLa cells was carried out using an MTT assay. As an important control experiment, the viability of cells cultured with polymeric vesicles without DOX·HCl was investigated, and it shows minor cytotoxicity at the concentration of copolymer in complete DMEM ranging from 15.6 to 250 mg/L. In comparison with blank polymeric vesicles, inclusion of DOX·HCl into these vesicles at the same concentration of copolymer exhibits significantly reduced cell viability of HeLa cells at concentrations above 31.3 mg/L (Figure 9). In particular, the viability decreases to <10% when the cells are incubated with DOX·HCl loaded vesicles at 250 mg/L.

Cellular Uptake of Polymeric Vesicles. The cellular uptake of the vesicles is an important aspect to assess the efficiency of this drug-delivery system (DDS). By using HeLa cell lines as the model in our study, the cellular uptake of fluorescein isothiocyanate (FITC)-labeled PzLL-SS-PEG-SS-PzLL polymeric vesicles 2 were analyzed qualitatively and quantitatively. The polymeric vesicles are fluorescein isothiocyanate (FITC)-labeled for fluorescent tracking. With regards to the qualitative aspect, the process of cellular uptake was monitored by fluorescence microscopy. Before the observation by CLSM, the cells were rinsed several times with DPBS to remove the excess vesicles outside of the cells. As the culture time increased from 30 min to 5 h, the FITC fluorescence inside the cells intensifies visually (Figure 10A), which is a clear evidence of the polymeric vesicles endocytosis into the tumor cells. Flow cytometry (FCM) measurements show a quantitative result. A 99.98% population of the cells were found to fast encapsulate FITC-labled polymeric vesicles, even with an incubation of only 30 min. As the incubation time

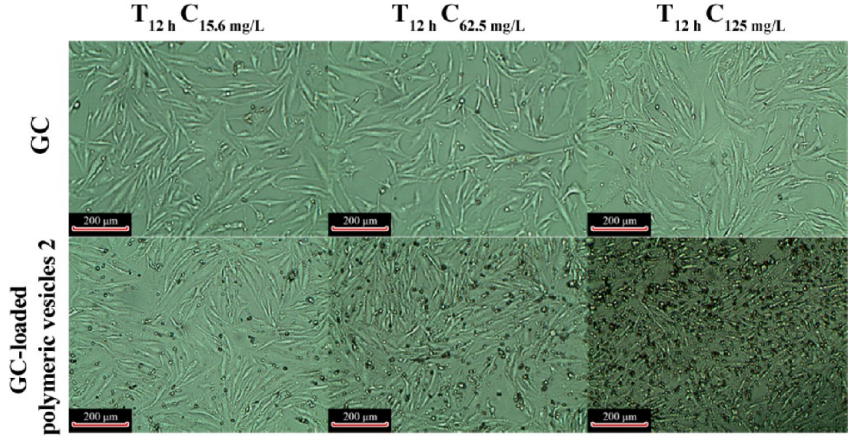

Figure 15. Representative microscope images of GC·HCl alone and GC·HCl-loaded PzLL-SS-PEG-SS-PzLL polymeric vesicles 2 after a 12 h coincubation with drug-resistant MDA-MB-231 cells.

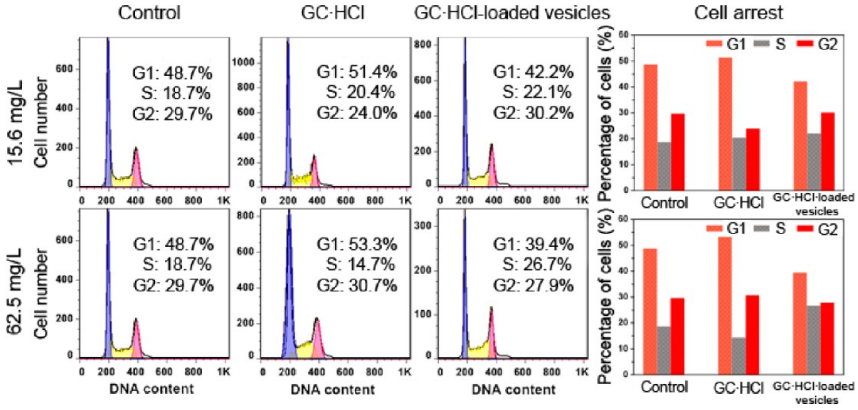

Figure 16. Cell cycle analyses of drug-resistant MDA-MB-231 cells treated with GC·HCl alone or GC·HCl-loaded PzLL-SS-PEG-SS-PzLL polymeric vesicles 2 for 12 h.

increases, the mean FITC fluorescence intensity gradually increases from 5.9 to 14.0 (Figure 10B), which implies that more polymeric vesicles are encapsulated by more cells.

Intracellular Release Regulated by the Reductive Environment. The redox-triggered disassembly of PzLL-SS-PEG-SS-PzLL polymeric vesicles is proposed to be the dominant drug-release mechanism in the previous experiments. We investigated how the redox-triggered mechanism that regulates the release of DOX·HCl affects the cell viability by MTT assay, and we observed the intracellular internalization of DOX·HCl by CLSM. To verify the triggering mechanism under different reduction conditions, exogenous GSH was added into fresh DMEM and incubated with the cells to increase the intracellular GSH concentration. Before the addition of the exogenous GSH, the cells were washed with DPBS several times to avoid the effect of the vesicles not being internalized into the cells. The cytotoxicity of the DOX·HCl-loaded PzLL-SS-PEG-SS-PzLL polymeric vesicles 2 in the presence and absence of GSH against HeLa cell lines was then carried out. Upon GSH treatment, the cells show an obvious decrease in viability. In contrast with cells without GSH treatment, cell viability of the group with GSH treatment shows a significant disparity, especially in the concentration range from 15.6 to 62.5 mg/L (Figure 11).

In a parallel study by CLSM observation (Figure 12), a similar phenomenon was observed for cells under the same incubation conditions with or without GSH. During the observation, it was found that the DOX·HCl (red) distribute all over the nucleus, as shown by the red fluorescence colocalizing with the blue nuclei stained by DAPI, especially in the GSH treatment group. As the concentration increases, the red fluorescence intensifies. Thus, the above results clearly support a redox-triggered drug-release mechanism.

Pathway of Cellular Uptake of Polymeric Vesicles by Drug-Resistant MDA-MB-231 Cells. MDR has been a tough barrier to successful chemotherapy in cancer. To assess the effects of these redox-responsive polymeric vesicles for overcoming MDR, we chose cell line MDA-MB-231, which is resistant to hydrophilic anti-breast-cancer drug GC·HCl. Like DOX·HCl, hydrophilic GC·HCl could be loaded into interior cavities of polymeric vesicles. We first studied the mechanism of cellular uptake of the polymeric vesicles. Currently, several pathways of nanoparticles endocytosis have been documented, including macropinocytosis, clathrin-dependent endocytosis, caveolin-dependent endocytosis, clathrin- and caveolin-independent endocytosis, and so forth. In this study, sodium azide (NaN_3), chlorpromazine, genistein, and colchicine were chosen as inhibitors for their corresponding endocytosis pathways. Figure 13 shows the marked decrease of cellular uptake of FITC-labelled PzLL-SS-PEG-SS-PzLL polymeric vesicles 2 in the sodium azide (NaN_3) group. This indicates that the cellular uptake was associated with an energy-dependent process because sodium azide can block cellular ATP synthesis. Additionally, genistein, which depolymerizes microtubules through the binding of tubulin, identifies another factor in this process because it also led to a decrease of the cellular uptake of FITC-labelled PzLL-SS-PEG-SS-PzLL polymeric vesicles 2. In sharp contrast, colchicine, which inhibits actin polymerization, shows a minimal effect on the cellular uptake, suggesting no correlation between cellular uptake with clathrin-mediated or caveolae-mediated endocytosis. A negligible alteration was also observed in the cellular uptake of vesicles in the presence of chlorpromazine, which interferes selectively with clathrin-mediated endocytosis. In all, the cellular uptake of polymeric vesicles is predominantly via energy-dependent and microtubule-dependent endocytosis.

Gemcitabine Hydrochloride (GC·HCl)-Induced Cytotoxicity by Polymeric Vesicles against Drug-Resistant MDA-MB-231 Cells. To demonstrate the role of polymeric vesicles in overcoming MDR, the cytotoxicity of GC·HCl alone, PzLL-SS-PEG-SS-PzLL polymeric vesicles 2 alone, and GC·HCl-loaded PzLL-SS-PEG-SS-PzLL polymeric vesicles 2 against drug-resistant MDA-MB-231 cells was carried out by using the MTT assay. GC·HCl-resistant MDA-MB-231 cells were produced by a repeated exposure to free GC·HCl until there was no obvious affect on their proliferation. As shown in Figure 14, the viability of MDA-MB-231 cells after exposure to GC·HCl over a wide concentration window results in no observable alteration. Furthermore, a slightly higher cell viability for the groups exposed to GC·HCl was observed at a lower concentration in comparison with the control, revealing the high resistance capability of MDA-MB-231. Importantly, synthetic material PzLL-SS-PEG-SS-PzLL polymeric vesicles 2 also exhibit low cytotoxicity to the drug-resistant MDA-MB-231 cells. In sharp contrast, the viability of cells cocultured with GC·HCl-loaded PzLL-SS-PEG-SS-PzLL polymeric vesicles is significantly reduced, supporting a positive role for the polymeric vesicles in overcoming MDR.

To demonstrate the positive effect in reversing MDR further, an experiment was carried out at three different concentrations

and monitored by general microscopy and flow cytometry (FCM). As shown in Figure 15, the GC·HCl-resistant MDA-MB-231 cells treated with GC·HCl for 12 h maintain their growth status over the whole range of the investigated concentrations, whereas the counterpart treated with GC·HCl-loaded polymeric vesicles presents an increasing mortality. This confirms that the polymeric vesicles play a key role in protecting GC·HCl from rapid metabolization to overcome MDR.

Cell Cycle Arrest in MDA-MB-231 Cells. GC·HCl can be transformed into its active metabolite by phosphorylation after its energy-dependent uptake. The metabolite then interacts with a replicating DNA strand, which will decrease the activity of DNA polymerase and inhibit DNA synthesis (S phase).[34] Theoretically, the ratio of cells in S phase will rise once GC·HCl plays a role in therapy. The DNA content histograms of the human breast cancer cell line MDA-MB-231 induced by free GC·HCl and GC·HCl-loaded polymeric vesicles at concentrations of 15.6 and 62.5 mg/L after a 12 h incubation are presented in Figure 16. The high concentration group (62.5 mg/L instead of 125 and 250 mg/L) was chosen because of the low viability of cells at both concentrations, which is not appropriate for FAC measurements. The results show that the ratio of MDA-MB-231 cells treated with GC·HCl-loaded polymeric vesicles arrested in S phase increases to 22.1 and 26.7% at the respective concentration of 15.6 and 62.5 mg/L. This verifies the role of the GC·HCl released from polymeric vesicles affecting the proliferation of MDA-MB-231 cells. In addition, a lower percentage of cells arrested in S phase for the GC·HCl treatment group (62.5 mg/L) was observed in comparison with the control. This might be correlated with the high resistance capability of MDA-MB-231 against GC·HCl, which is in line with the results shown in the cytotoxicity study.

4. CONCLUSIONS

This study focuses on disulfide-bridged copolymer PzLL-SS-PEG-PzLL vesicles as a novel hydrophilic anticancer drug-delivery system for overcoming MDR. We selected drug-sensitive cells and drug-resistant cells to research drug release and localization and the effect on overcoming MDR, respectively. The results show the significantly increased accumulation of hydrophilic drugs in the nucleus under a reducing environment in drug-sensitive cancer cells as well as the enhanced cytotoxicity of drugs in drug-resistant cancer cells. In addition, the multifunctional vesicles enhance the bioavailability of anticancer drugs because they can load hydrophilic drugs. These findings imply that PzLL-SS-PEG-SS-PzLL vesicles may be engineered into promising vehicles for the delivery of chemotherapeutic agents for overcoming multidrug resistance, to some extent, in cancer therapy.

■ ASSOCIATED CONTENT

Supporting Information

Morphology of PzLL-SS-PEG-SS-PzLL (W_{PEG}/W_{PzLL} 1:2) vesicles with different sizes determined by TEM, morphology of DOX·HCl-loaded PzLL-SS-PEG-SS-PzLL (W_{PEG}/W_{PzLL} 1:2) vesicles triggered by GSH determined by TEM, and image of DOX·HCl-loaded vesicles samples after drug release with and without GSH. This material is available free of charge via the Internet at http://pubs.acs.org.

■ AUTHOR INFORMATION

Corresponding Author

*E-mail: yongyong_li@tongji.edu.cn.

Notes

The authors declare no competing financial interest.

■ ACKNOWLEDGMENTS

This work was financially supported by the National Natural Science Foundation of China (21004045, 51173136, and 21104059), Shanghai Rising-Star Program (12QA1403400), "Chen Guang" project founded by the Shanghai Municipal Education Commission and Shanghai Education Development Foundation, and the State Key Laboratory of Molecular Engineering of Polymers (Fudan University, K2011-04).

■ REFERENCES

(1) Wu, C. P.; Hsieh, C. H.; Wu, Y. S. *Mol. Pharm.* **2011**, *8*, 1996–2011.
(2) Kuhn, N. Z.; Nagahara, L. *Mol. Pharm.* **2011**, *8*, 1994–1995.
(3) Pan, L. M.; Liu, J. A.; He, Q. J.; Wang, L. J.; Shi, J. L. *Biomaterials* **2013**, *34*, 2719–2730.
(4) Kong, D. J.; Ma, S. M.; Liang, B.; Yi, H. Q.; Zhao, Y. L.; Xin, R.; Cui, L.; Jia, L. L.; Liu, X.; Liu, X. D. *Biomed. Pharmacother.* **2012**, *66*, 271–278.
(5) Ke, C. J.; Chiang, W. L.; Liao, Z. X.; Chen, H. L.; Lai, P. S.; Sun, J. S.; Sung, H. W. *Biomaterials* **2013**, *34*, 1–10.
(6) Chen, Y. T.; Chen, C. H.; Hsieh, M. F.; Chan, A. S.; Liau, I.; Tai, W. Y. In 13th International Conference on Biomedical Engineering, Singapore, Dec 3–6, 2008; Lim, C. T.; Goh Cho Hong, J., Eds.; Springer: New York, 2009; Vol. *23*, pp 1224–1227.
(7) Brigger, I.; Dubernet, C.; Couvreur, P. *Adv. Drug Delivery Rev.* **2012**, *64*, 24–36.
(8) Li, P. Y.; Lai, P. S.; Hung, W. C.; Syu, W. J. *Biomacromolecules* **2010**, *11*, 2576–2582.
(9) Attia, A. B. E.; Yang, C.; Tan, J. P. K.; Gao, S. J.; Williams, D. F.; Hedrick, J. L.; Yang, Y. Y. *Biomaterials* **2013**, *34*, 3132–3140.
(10) Aryal, S.; Hu, C. M.; Zhang, L. *Mol. Pharm.* **2011**, *8*, 1401–1407.
(11) Meng, F. H.; Zhong, Z. Y.; Feijen, J. *Biomacromolecules* **2009**, *10*, 197–209.
(12) Osada, K.; Christie, R. J.; Kataoka, K. *J. R. Soc., Interface* **2009**, *6*, 325–339.
(13) Onaca, O.; Enea, R.; Hughes, D. W.; Meier, W. *Macromol. Biosci.* **2009**, *9*, 129–139.
(14) Du, J.; O'Reilly, R. K. *Soft Matter* **2009**, *5*, 3544–3561.
(15) Wang, Y. C.; Wang, F.; Sun, T. M.; Wang, J. *Bioconjug. Chem.* **2011**, *22*, 1939–1945.
(16) Oh, K. T.; Yin, H. Q.; Lee, E. S.; Bae, Y. H. *J. Mater. Chem.* **2007**, *17*, 3987–4001.
(17) Wen, H. Y.; Dong, H. Q.; Xie, W. J.; Li, Y. Y.; Wang, K.; Pauletti, G. M.; Shi, D. L. *Chem. Commun.* **2011**, *47*, 3550–3552.
(18) Dembereldorj, U.; Kim, M.; Kim, S.; Ganbold, E. O.; Lee, S. Y.; Joe, S. W. *J. Mater. Chem.* **2012**, *22*, 23845–23851.
(19) Franco, R.; Cidlowski, J. A. *Cell Death Differ.* **2009**, *16*, 1303–1314.
(20) Meng, F.; Hennink, W.E.; Zhong, Z. *Biomaterials* **2009**, *30*, 2180–2198.
(21) Cerritelli, S.; Velluto, D.; Hubbell, J.A. *Biomacromolecules* **2007**, *8*, 1966–1972.
(22) Cai, X.-J.; Dong, H.-Q.; Xia, W.-J.; Wen, H.-Y.; Li, X.-Q.; Yu, J.-H.; Li, Y.-Y.; Shi, D.-L. *J. Mater. Chem.* **2011**, *21*, 14639–14645.
(23) Ren, T. B.; Xia, W. J.; Dong, H. Q.; Li, Y. Y. *Polymer* **2011**, *52*, 3580–3586.
(24) Li, M. H.; Keller, P. *Soft Matter* **2009**, *5*, 927–937.
(25) Ren, T. B.; Liu, Q. M.; Lu, H.; Liu, H. M.; Zhang, X.; Du, J. Z. *J. Mater. Chem.* **2012**, *22*, 12329–12338.

(26) Cai, X.; Dong, C.; Dong, H.; Wang, G.; Pauletti, G. M.; Pan, X.; Wen, H.; Mehl, I.; Li, Y.; Shi, D. *Biomacromolecules* **2012**, *13*, 1024−1034.
(27) Dong, H. Q.; Li, Y. Y.; Wen, H. Y.; Xu, M.; Liu, L. J.; Li, Z. Q.; Guo, F. F.; Shi, D. L. *Macromol. Rapid Commun.* **2011**, *32*, 540−545.
(28) Chu, M.; Dong, C.; Zhu, H.; Cai, X.; Dong, H.; Ren, T.; Su, J.; Li, Y. *Polym. Chem.* **2013**, *4*, 2528−2539.
(29) Wen, H.; Dong, C.; Dong, H.; Shen, A.; Xia, W.; Cai, X.; Song, Y.; Li, X.; Li, Y.; Shi, D. *Small* **2012**, *8*, 760−769.
(30) He, C. B.; Hu, Y. P.; Yin, L. C.; Tang, C.; Yin, C. H. *Biomaterials* **2010**, *31*, 3657−3666.
(31) Deming, T. J. *Adv. Mater.* **1997**, *9*, 299−311.
(32) Kramer, J. R.; Deming, T. J. *Biomacromolecules* **2010**, *11*, 3668−3672.
(33) Pickel, D. L.; Politakos, N.; Avgeropoulos, A.; Messman, J. M. *Macromolecules* **2009**, *42*, 7781−7788.
(34) Hosseinzadeh, H.; Atyabi, F.; Dinarvand, R.; Ostad, S. N. *Int. J. Nanomed.* **2012**, *7*, 1851−1863.